nature geoscience
SUPPLEMENTARY INFORMATION
DOI: 10.1038/NGEO1829

(Chen et al., Contribution of polar and mountain glacier melt to recent sea level rise)

1. Steric Sea Level Changes From Argo Data

The Argo floats network consists of a large collection of small, drifting oceanic robotic probes deployed worldwide, and can measure sea water properties (including temperature, salinity, and pressure) from the surface to a depth of ~ 2000 m. This is a joint project of large group of countries. The Argo floats started to be deployed in around year 2000, and has reached the pre-designed stable amount of probes (around 3200) since November 2007. Ideally, people should use Argo data for the period since 2007 to do global analysis, because of the good and consistent global coverage. However, in the mean time, people also want to get an Argo record as long as possible to examine long-term variability of the ocean (e.g., steric sea level change).

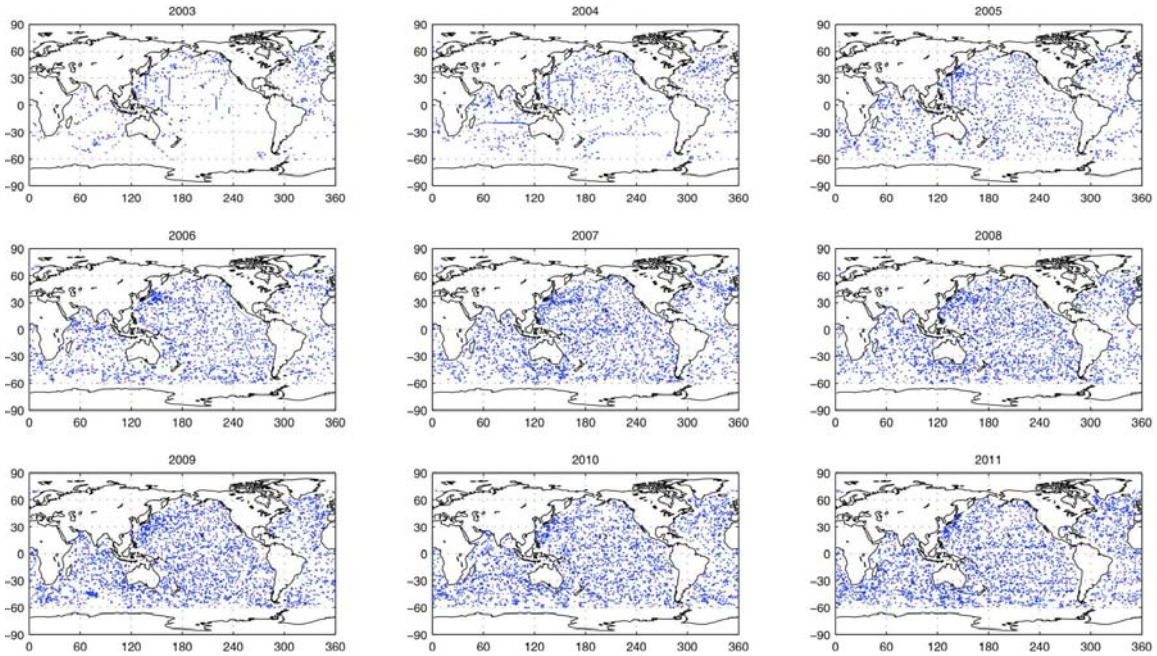

Figure S1. Global distribution of Argo floats in January of each year from 2003 through 2011.

In this study, we only use the Argo data covering January 2005 to December 2011, which is based on the fact that the spatial coverage of available Argo floats in the early years (2000 – 2004) is not sufficient enough for doing global analysis, especially for the southern hemisphere. Fig. S1 shows the spatial distribution of Argo floats in January of each year from 2003 through 2011. Although some previous studies[S1,S2] use Argo data for the periods as early as 2003 to estimate global mean steric sea level change, it is obvious that large uncertainty is expected for those early years' data, as the numbers of observations during those periods are simple not enough, especially for the southern oceans.

Three different global gridded monthly Argo temperature (T) and salinity (S) datasets covering the period from January 2005 through December 2011 are used in this study, which include the global gridded T and S fields provided by the International Pacific Research Center (IPRC) at the University of Hawaii, Japan Agency for Marine-Earth Science and Technology (JAMSTEC or denoted as JAMS in plots and tables), and Scripps Institution of Oceanography (SIO) at the University of California at San Diego (more descriptions of these Argo data products are available at http://www.argo.ucsd.edu/Gridded_fields.html). Steric sea level change is computed for each grid point on 1ºx1º grids using Argo T, S, and pressure data. Global mean steric sea level changes are estimated by averaging the steric rate at each grid point with cosine of latitude as weighting, and the three time series are shown in Fig. S3a. After seasonal, i.e. annual and semiannual variations have been removed, there is a clear increasing trend in all three time series (Fig. S3b), with estimated rates of 0.48 ± 0.22, 0.78 ± 0.35, 0.54 ± 0.22 mm/yr for the IPRC, JAMS, and SIO estimates, respectively. The average rate of the three time series is ~ 0.60 ± 0.27 mm/yr over the studied period (2005-2011). The uncertainties are estimated based on unweighted least squares linear fits to each series using a Monte Carlo method with 95% confidence (see Section 4 for details on uncertainty estimation).

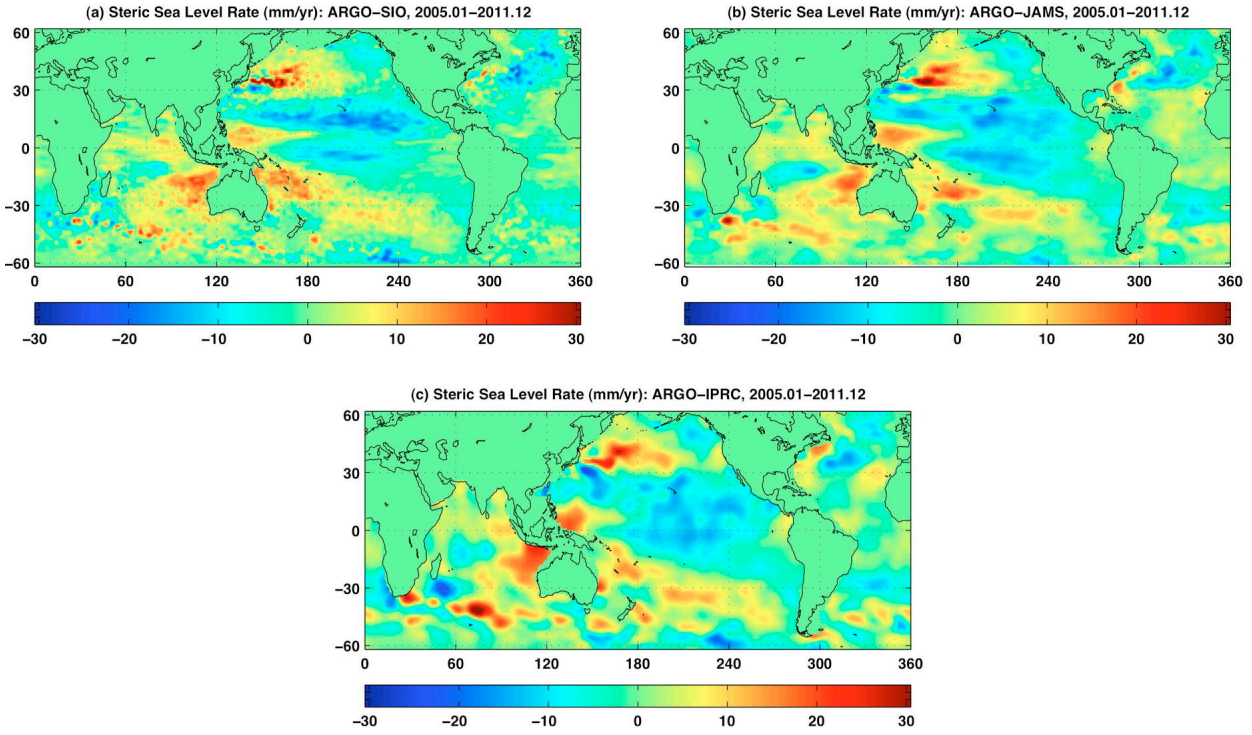

Figure S2. Maps of global long-term steric sea level rates (in mm/yr) over the period Jan. 2005 to Dec. 2011, estimated from the SIO, JAMS, and IPRC Argo datasets. Aside from the largely consistent spatial patterns, discrepancies are also evident, especially in the southern oceans.

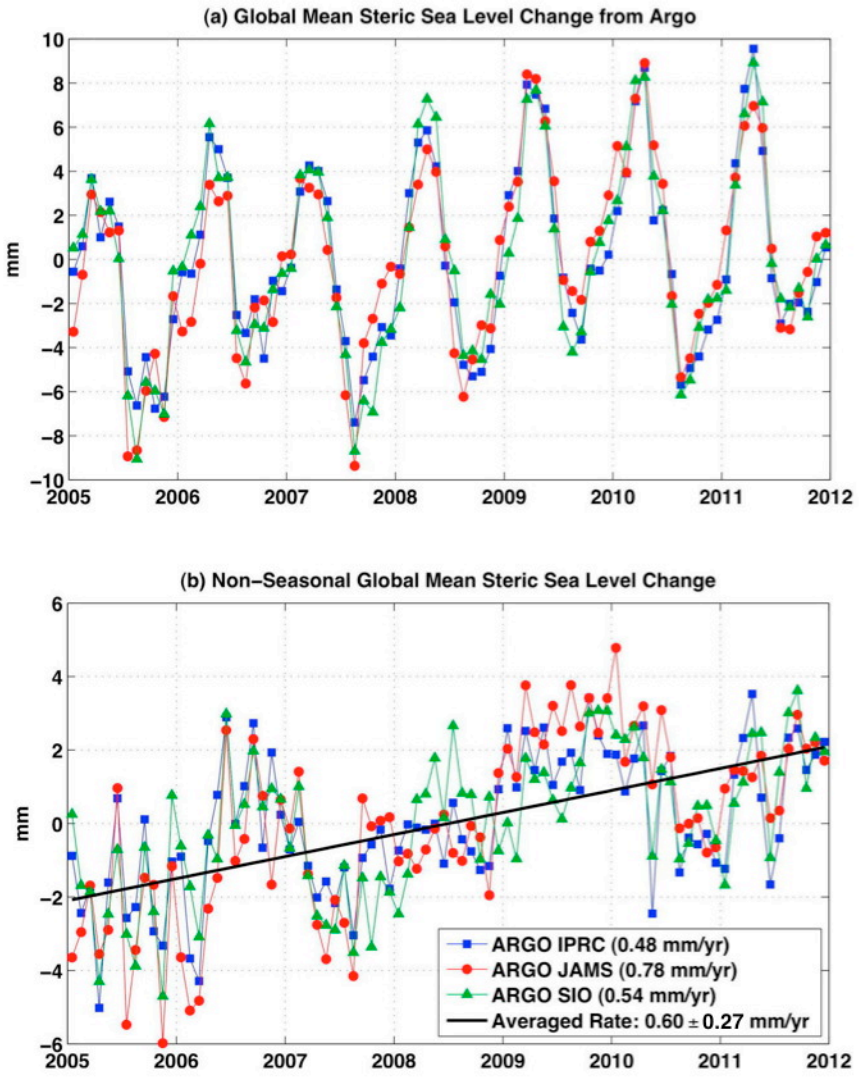

Figure S3. a) Global mean steric sea level change during 2005 and 2011, estimated from three global gridded Argo datasets (IPRC, JAMS, and SIO). b) Same as in a), but seasonal (including annual and semiannual) variations have been removed using unweighted least squares fit. The thick black line represents the mean linear trend of the three time series.

2. Global Mean Sea Level Change and NINO 3.4 Index

It is a well known fact that the global mean sea level is closely correlated to El Niño and La Niña events[S3-S5]. During the period 2005 to 2011, the global mean sea level rate observed by Jason-1/2 satellite altimeters is ~ 2.39 ± 0.48 mm/yr (see Fig. S4a), which is considerably smaller than average rate of ~ 3.13 ± 0.40 mm/yr over a longer period 1993 to 2011, covered by both TOPEX/Poseidon (T/P) and Jason-1/2 satellite altimeters. During the recent period (2005-2011), the global mean sea level shows significantly larger interannual variability, featured by two very obvious sea level drops (marked by green dashed circles in Fig. S4a) during the 2007/2008 and

2010/2011 time periods. These two drops in the global mean sea level correspond to two major La Niña events during the same periods (see Fig. S4b).

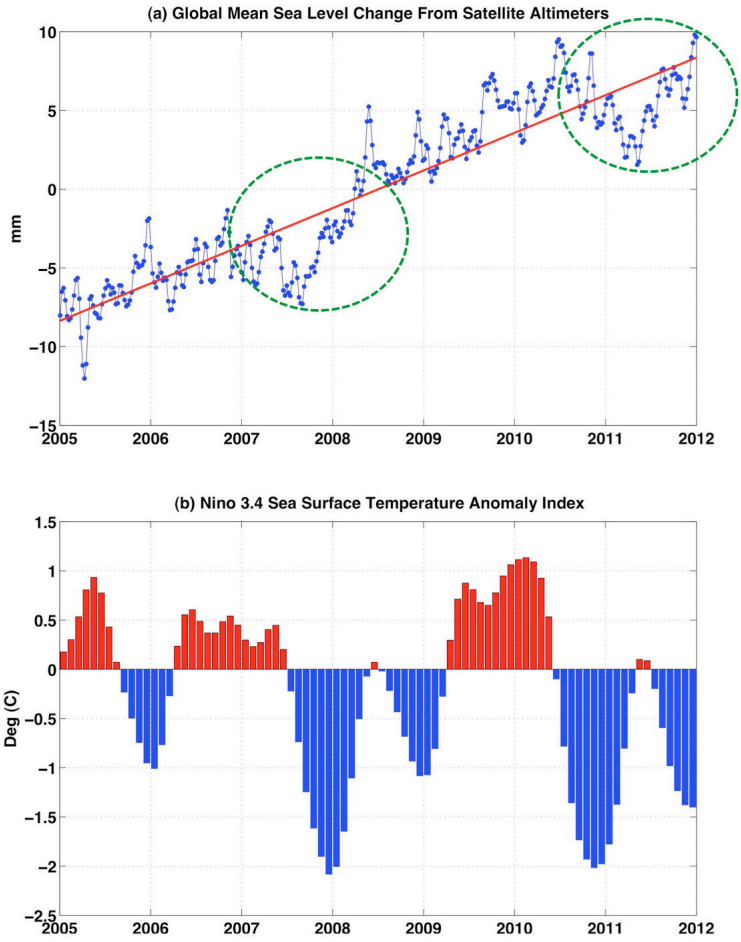

Figure S4. Comparison of (a) Jason-1/2 satellite altimeters observed global mean level change and (b) the NINO 3.4 sea surface temperature (SST) anomaly index over the period January 2005 to December 2011. Seasonal (including annual and semiannual) variations have been removed from Jason-1/2 altimeters sea level time series using unweighted least squares fit. The red line represents the linear trend estimated from least squares fit. A five-month moving average has been applied to the NINO 3.4 SST anomaly index time series.

3. Global Mean Oceanic Mass Rates From GRACE

3.1 Apparent Mass Rates from GRACE

GRACE RL05 monthly gravity solutions over the period January 2005 and December 2011, provided by the Center for Space Research (CSR), University of Texas at Austin, and Geschossflächenzahl (GFZ), Potsdam are used to estimate global mean oceanic mass rate, or mass contribution to the global sea level rise. At high degrees and orders, GRACE spherical harmonics are contaminated by noise, including longitudinal stripes, and other errors. The very

low degree, especially the degree-2 coefficients in GRACE solutions are also subject to relatively large uncertainty. In order suppress spatial noise in GRACE-derived mass fields, a decorrelation filter and 500 km Gaussian smoothing are applied. A global gridded (1° x 1°) surface mass change field is calculated from each of the GRACE monthly spherical harmonic solutions, under three different cases: 1) replacing GRACE degree-2 zonal C_{20} coefficients with satellite laser ranging (SLR) estimates, 2) replacing GRACE all degree-2 coefficients (including C_{20}, C_{21}, S_{21}, C_{22}, S_{22}) with SLR estimates, 3) GRACE data only. The SLR degree-2 spherical harmonics are derived based on the same GRACE RL05 standards. The PGR effect on GRACE data is removed using an updated version of the Paulson07 PGR model (noted as Geruo13), which has corrected the error introduced by accidentally neglecting the rotational feedback effect in the Paulson07 model[S6]. The difference between the Paulson07 and Paulson12 models (in terms of contribution to global mean oceanic mass rate) is minimal, at only ~ 10% of model prediction.

At each grid point, we fit the mass change time series with a linear trend, plus annual, semiannual via unweighted least squares. The slope of the linear trend at a particular location is an estimate of apparent surface mass rate. The apparent rate will generally differ from the true rate due to spatial leakage and biases associated with filtering and processing. Figure S5 shows global apparent mass rates (in units of cm/yr equivalent water height) for the period January 2005 to December 2011, derived from CSR RL05 GRACE solutions.

3.2 Recovering "True" Oceanic Mass Rates

The map of apparent mass rates shows the effects of spatial filtering and a limited range of spherical harmonics. Both produce leakage of variance, so that any localized storage changes are spread to adjacent areas (Fig. S5a), with significant amplitude attenuation. It is possible to correct for these leakage and bias effects because their underlying causes (spatial filtering and limited harmonic range) are known. Previous studies[S7-S9] have demonstrated that forward modeling provides an effective method to correct for leakage and bias in GRACE estimates of regional mass change rate. The basic concept has been implemented by using geographical and other information to identify likely locations of mass changes within a region, and then adjust amplitudes so that after spherical harmonics truncation and spatial filtering are applied, the results agree with GRACE apparent rates. In the present study, we extend the regional forward modeling method to global scale, using a 'no-constraint' modeling scheme for the entire Earth surface. We define a global 1°x1° grid and allow each grid area to contribute to the GRACE apparent mass rate map (Fig. S5a). In an iterative process, mass rates are assigned to each grid point on land (including ice sheets and mountain glaciers), and then subjected to the same processing steps used to produce Fig. S5a, including spatial filtering and truncation of spherical harmonics. At any given time step, a layer of water is evenly distributed over the ocean, negatively equaling the total of mass rates over land (sum of all points over land with cosine of latitude as weighting). This is equivalent to assuming that 1) mass rate over the ocean is spatially constant at a given time step, and 2) the total mass on the Earth surface is conserved.

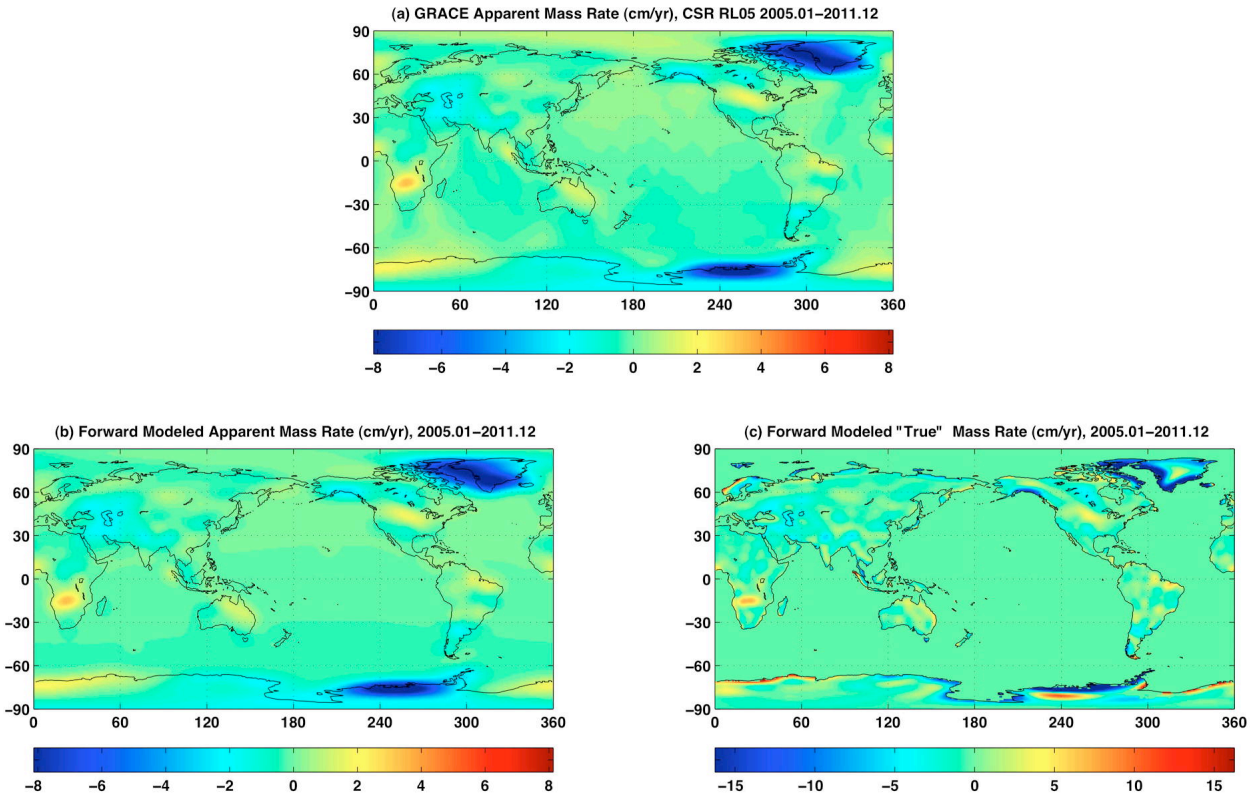

Figure S5. a) Global apparent mass rates estimated from GRACE CSR RL05 monthly gravity solutions over the period 2005-2011. A decorrelation filter and 500 km Gaussian smoothing are applied to GRACE data. PGR effect is removed using the Paulson12 (an updated version of Paulson07) PGR model, and the GRACE C_{20} coefficients are replaced by SLR solutions. b) Forward modeled apparent mass rates (that are produced from the "true" mass rates shown in panel c after truncations and spatial filterings). c) Forward modeled "true" mass rates, which are the reconstructed "true" global mass rates after 65 iterations.

The global forward modeling includes the following steps:

1) At each grid point on a 1°x1° grid, a trial mass rate is assigned equal to the GRACE apparent mass rate (in Fig. S5a). Ocean areas are assigned with a uniform layer of water, negatively equaling to the total mass rate over land.

2) A forward model apparent mass rate map (Fig. S5b) is obtained by representing the 1º x 1º gridded model mass rates from Step 1 in fully normalized spherical harmonics, truncated at degree and order 60. The degree 0 and 1 coefficients are set to zero. Then the 500 km Gaussian smoothing filter is applied and the result is compared with Fig S5.

3) At each grid point, the difference between GRACE apparent rate (Fig. S5a) and modeled apparent rate (Fig. S5b) is added to the model rate with a scale factor of 1.2 (to speed up the convergence). The new model rate is filtered as in Step 2, and the process repeated. Successive iterations produce increasing agreement between modeled and GRACE apparent rate maps.

4) We stop iterations when the difference between modeled mean oceanic mass rates from two consecutive interactions falls below a specified value, or when the modeled mean oceanic mass rate reaches a maximum value.

The reconstructed 'true' global mass rate map (Fig. S5c), which after going through similar spatial filtering and truncation (and other data processing procedures) as used in GRACE data, will generate a modeled apparent global rate map (Fig. S5b) that well resembles GRACE observations (Fig. S5a). In this particular example (CSR RL05, deccorelation filtering + 500 km Gaussian smoothing, C_{20} from SLR), the global mean oceanic mass rate is estimated to be ~ 1.75 mm/yr, which is significantly larger than the estimated rate of ~ 0.98 mm/yr from using a ocean function with 600km buffer zone (excluding coastal ocean areas within 600 km distance from the coastline). We estimate global mean ocean mass rates via the global forward modeling from two RL05 solutions (CSR and GFZ), with three different treatments of GRACE degree-2 gravity coefficients. Results from the six cases are summarized in Table S1.

Table S1. Mass rates from the two RL05 data sets and three treatments of degree 2 SH coefficients as described in the text for the period 2005-2011. The far right column (Ocean) corresponds to the Table 1 Mass column showing published estimates. Separate rates are also given for Antarctica, Greenland, mountain glaciers, and all other TWS sources combined (all are in equivalent mass rates over the global ocean). The uncertainties are estimated by considering formal error in GRACE mass rates (with 95% confidence interval), and standard deviations among the six GRACE estimates, potential PGR model error over the Antarctica, and long-term geocenter effect on global mean sea level are also considered (see SI for details on uncertainty assessments).

GRACE Estimates	Antarctica (mm/yr)	Greenland (mm/yr)	Glacier (mm/yr)	TWS (mm/yr)	Ocean (mm/yr)
CSR RL05 + SLR C20	-0.51	-0.69	-0.53	-0.01	1.75
CSR RL05 + SLR Degree-2	-0.52	-0.68	-0.53	+0.02	1.71
CSR RL05, No SLR	-0.67	-0.74	-0.63	-0.13	2.17
GFZ RL05 + SLR C20	-0.48	-0.67	-0.52	+0.18	1.49
GFZ RL05 + SLR Degree-2	-0.39	-0.67	-0.54	-0.64	2.24
GFZ RL05, No SLR	-0.46	-0.67	-0.50	+0.19	1.44
Mean GRACE estimates and uncertainties	-0.50 ± 0.26	-0.69 ± 0.05	-0.54 ± 0.10	-0.07 ± 0.32	1.80 ± 0.47

4. Uncertainty Assessment

4.1 Uncertainty of Altimetry Estimates

Slope estimates from sea level and related time series are from unweighted least squares linear fits to each series. Uncertainty in slope estimates arises from two fundamental causes. One is measurement errors in individual time series, which may be presumed independent from one sample to the next and Normally distributed. A much larger cause of uncertainty is

superimposed low frequency residual signals, from El Nino events and other sources, causing deviations from linearity that are correlated from one sample to the next, and not independent. We use a Monte Carlo method to assess slope uncertainty, which effectively considers both causes. We generate an ensemble of 10,000 synthetic time series in which each ensemble member is the sum of a linear trend (with known slope equal to estimated slope), plus a random residual time series which has, on average, the same auto-correlation properties as the observed residual. Ensemble residual series are generated in the frequency domain, using Gaussian pseudo-random numbers for real and imaginary parts at each frequency, scaled to give the same average Fourier power spectrum as the observed residual. A histogram of the 10,000 estimates shows them to be approximately Normally distributed (Fig. S6), with plus and minus two standard deviations providing a 95% confidence interval.

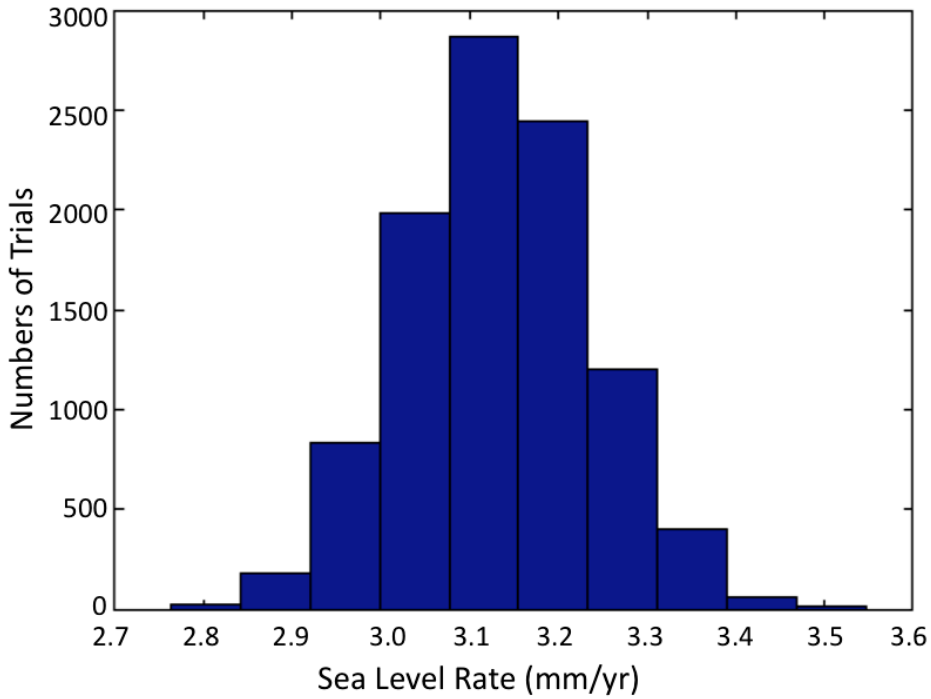

Figure S6. Histogram of estimated linear trends of the 19-years altimetry sea level time series from the 10,000 trials in the Monte Carlo test.

Based on the method described above, the estimated mean sea level rates for the 19-years (1993-2011) and 7-years (2005-2011) altimetry time series (shwon in Fig. 1a & 1b) are 3.13 ± 0.22 mm/yr and 2.39 ± 0.48 mm/yr, respectively (seasonal signals, i.e., annual and semiannual variations have been removed from the altimtry time series first, using unweighted least squares fit). These uncertainties (± 0.22 and ± 0.48 mm/yr) only represent the formal errors from the two altimetry time series with 95% confidence. Many other factors can also affect the uncertainty of altimtry estimates, including the non-global coverage of T/P and Jason-1/2 satellite altimeters

(which only cover 66ºS-66ºN), potential altimter bias and/or drift with respect to tide gauge data, errors in geophysical model corrections, and etc.. A more realistic uncertainty for the altimeter global sea level rate (over the entire time span 1993 – present) is estimated to be ~ ± 0.4 mm/yr [8]. Therefore, we adopt this estimate as the error bound for the 19-years sea level rate (3.13 ± 0.40 mm/yr; see Fig. 1a). For the 7-years rate, we neglect other error sources, and use the formal error with 95% confidence to approximate the error bound (assuming other errors when considered will not change the conclusion).

4.2 Uncertainty of Argo Estimates

The Argo steric sea level time series also show significant interannual variability (see Fig. S3), which affects the estimation of uncertainty using conventional treatments of slope uncertainty. Here, we use the same Monte Carlo approach (as used in altimeter data). The estimated rates and uncertainties (with 95% confidence) for the IPRC, JAMS, and SIO Argo time series are 0.48 ± 0.22, 0.78 ± 0.35, 0.54 ± 0.22 mm/yr, respectively. The average rate and uncertainty of the three Argo results can be estimated in two ways. One is using simple average of the three estimates, which gives 0.60 ± 0.16 mm/yr. Another approach is to fit a slope to all the data (including IPRC, JAMS, and SIO) using the Monte Carlo method, which gives 0.60 ± 0.25 mm/yr (with 95% confidence). We use the latter (± 0.25 mm/yr) as a safer bound of formal error. The Argo data only cover the the top 2000 m of the ocean. The deep ocean (below 2000 m) may have non-negligible contribution of up to ± 0.1 mm/yr to global sea level rate[S10]. After this pontential error is considered, the average Argo global steric sea level rate is estimated to be 0.60 ± 0.27 mm/yr.

4.3 Uncertainties of GRACE Estimates

The uncertainties of GRACE estimates are computed from the following four contributions: formal error of GRACE mass rates from the least squares fit (with 95% confidence), standard deviation among the six GRACE estimates, potential PGR model error, and potential geocenter effect. As the forward modeling method deals with GRACE mass rate maps (i.e., apparent, modeled, and "true" rate maps as shown in Fig. S5), not time series, computation of formal error is more challenging. When we compute the GRACE apparent mass rate map (e.g., the one shown in Fig. S5a) for each of the six GRACE estimates, a corresponding uncertainty (with 95% confidence) map is also also computed using least squares fit. We take the mean ratios between uncertainties and the estimated rates for each of the five studied regions (i.e., Antarctica, Greenland, Mountain Glaciers, Land Water, and Ocean) as the approximate percentages between formal errors and GRACE estimated mass rates from forward modeling (as listed in Table 2). We first compute regional means from each of the six GRACE estimates, and then take the average of the six mean ratios as the mean error percentage (for that region). The estimated error percentages for Antarctica, Greenland, Mountain Glaciers and Land Water, are ~

~ 20%, 6%, 16%, and 53%, respectively (the ocean estimates equal to the negative sum of the four regions). These translate into ± 0.10, ± 0.04, ± 0.09, ± 0.04 mm/yr for the Antarctic, Greenland, Mountain Glaciers and Land Water (TWS) estimates.

PGR models' error will also affect GRACE estimated mass rates, especially over the Antarctic ice sheet[S11,S12]. The true uncertainty of PGR models is virtually unknown, because of the lack of *in situ* measurements to contrain the models. As the focus of the present study is to reduce leakage error in GRACE estimated mass rates, an thorough analysis of PGR model errors is beyond the scope of this study. We adopt a published estimate (~ ± 79 Gt/yr)[S11] to approximate potential PGR model error over Antarctica, which gives ~ ± 0.21 mm/yr on global mean sea level contribution. PGR model error in other regions is a less concern, and likely within the estimated error bounds (from other sources).

Long-term geocenter (i.e., the center of mass of the Earth eystem) motion can be another error source to GRACE estimates. GRACE gravity solutions are defined in a reference frame that uses the center of mass as the origin. Therefore, theoretically geocenter motion, or the degree-1 spherical harmonic term does not exist in GRACE solution (or in another word, geocenter is "fixed" in the GRACE reference frame). The same applies to the PGR model mentioned above, which is also defined in the mass center reference frame. However, surface mass reidtribution within the Earth system will indeed introduce changes of geocenter, with respect to the terrestrial reference frame (fixed on the Earth crust). Consideration potential geocenter motion effect in GRACE estimates is complicated and difficult, because of the involvement of reference issue and also the relatively large uncertainty of long-term geocenter motion derived from geodetic observations.

Here, we estimate potential long-term geocenter motion effect on GRACE estimated ocean mass rates using two recently published results (those related to present-day mass) based on joint inversion of GRACE, and GPS, and satellite altimeter data[S13.S14]. The estimated contributions to global mean sea level rate is about 0.05 and 0.2 mm/yr, when using the two published geocenter rates, (-0.08, 0.29, and -0.16 mm/yr)[S13], or (-0.14, 0.12, and -0.37 mm/yr)[S14] for the X, Y, and Z components. We use 0.2 mm/yr as likely upper error bound of potential geocenter effect and include this in the error budget for GRACE estimated mean global sea leve rate (1.80 ± 0.47 mm/yr).

We have also examined potential effect on GRACE estimated sea level rates due to the consideration of self-gravitation. Based on a simplified point-mass self-gravitation model[S15], we allocate 100 Gt/yr ice loss in southern Greenland, and distribute the ice loss over the global ocean in two cases, with or without considering self-gravitation. We convert the constructed mass rate models into gravity fields, and apply 500 km Gaussian smoothing to the converted gravity fields back to mass rate fields (the so called apparent mass rate maps). We the apply the same forward modeling method to recover the "true" mass rate over southern Greenland (see Fig. S7). Apparently, self-gravitation has almost no notable impact on the recovered mass rates. This is not a surprise, as the main purpose of forward modeling is to reduce the leakage between land

and ocean, and as long as the method can effectively remove leakage error, it will effectively recover the "true" mass rates over land (-99.8 Gt/yr recovered vs. -100 Gt/yr ground truth after 40 iterations in this particular experiment), although self-gravitation will still affect how will the melt water spatially distribute over the ocean (but not the total amount of melt water going into the ocean, which is the key quantity the forward modeling can recover accurately). In the present study, potential loading effect on ocean mass redistribution is not considered, which may also affect GRACE estimated ocean mass rate[S16].

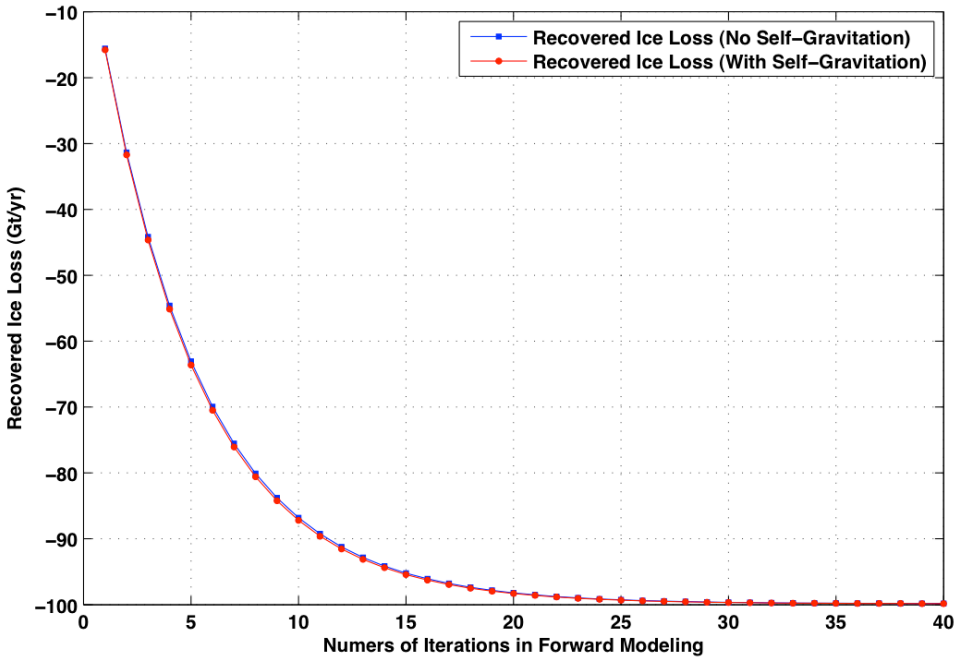

Figure S7. Recovered ice losses over southern Greenland with or without the consideration of self-gravitation effect.

The different spatial coverages of GRACE, Argo, and satellite altimetry data can also affect the closure of the global mean sea level budget. The Jason-1/2 altimeters data only cover the global ocean between 66ºS-66ºN, while GRACE covers almost the entire Earth surface. Although Argo data cover the similar regions as altimeter observations, the Argo floats typically do not sample shallow water and coastal regions and some other areas (e.g., Indonesia) that have experienced high rates of wind-driven sea level rise. This may be a source of sampling error in the Argo results. If we directly sum up GRACE observed mass change over the entire ocean, and compare with altimetry and Argo data, the extra contribution in the Arctic ocean in GRACE data may introduce some discrepancy. In the case of using CSR RL05 solution (with C_{20} replaced by SLR estimates), the inclusion of the Arctic ocean introduces an effect of only ~ 0.07 mm/yr on global sea level rate, well below the estimated error bound (± 0.47 mm/yr). Furthermore, the approach used in the present study is to estimate mass rates over the land (not directly over the

ocean) using forward modeling, in which melt water is evenly distributed over the global ocean. Therefore, including Arctic or not will not affect the estimated average mass rate over the ocean from the forward modeling (as the ocean has a uniform sea level rate everywhere).

References and Notes:

S1. Lombard, A., et al., Estimation of steric sea level variations from combined GRACE and Jason-1 data, *Earth and Planetary Science Letters* 254, 194–202, doi:10.1016/j.epsl.2006.11.035 (2007).

S2. Willis, J. K., Chambers, D. P., and Nerem, R. S., Assessing the globally averaged sea level budget on seasonal to interannual timescales, *J. Geophys. Res*., 113, C06015, doi:10.1029/2007JC004517 (2008).

S3. Ngo-Duc, T., Laval, K., Polcher, J., and A. Cazenave A., Contribution of continental water to sea level variations during the 1997–1998 El Niño–Southern Oscillation event: Comparison between Atmospheric Model Intercomparison Project simulations and TOPEX/Poseidon satellite data, *J. Geophys. Res*., 110, D09103, doi:10.1029/2004JD004940 (2005).

S4. Nerem, R., Chambers, D., Choe, C., and Mitchum, G., Estimating Mean Sea Level Change from the TOPEX and Jason Altimeter Missions. *Marine Geodesy*, 33(1 supp 1), 435-446. doi:10.1080/01490419.2010.491031 (2010).

S5. Boening, C. *et al.,* The 2011 La Niña: So strong, the oceans fell, *Geophys. Res. Lett.*, 39, L19602, doi:10.1029/2012GL053055 (2012).

S6. Geruo, A., Wahr, J., and S. Zhong, S., Computations of the viscoelastic response of a 3-D compressible Earth to surface loading: an application to Glacial Isostatic Adjustment in Antarctica and Canada, Geophys. J. Int., 192, 557–572, doi: 10.1093/gji/ggs030 (2013).

S7. Chen, J. L., Wilson, C. R., Tapley, B. D, Satellite Gravity Measurements Confirm Accelerated Melting of Greenland Ice Sheet, *Science*, Vol. 313 no. 5795 pp. 1958-1960, DOI: 10.1126/science.1129007 (2006).

S8. B. Wouters, B., Chambers, D. P., Schrama, E. J. O., GRACE observes small-scale mass loss in Greenland, *Geophys. Res. Lett.,* 35, L20501, doi:10.1029/2008GL034816 (2008).

S9. Chen, J. L., Wilson, C. R., Blankenship, D. D., Tapley, B. D, Accelerated Antarctic ice loss from satellite gravity measurements, *Nature Geosciences*, 2, 859 – 862, DOI:10.1038/NGEO694 (2009).

S10. Purkey, S. G., and Johnson, G. C., Warming of Global Abyssal and Deep Southern Ocean Waters between the 1990s and 2000s: Contributions to Global Heat and Sea Level Rise Budgets, *J. Climate*, 23, 6336-6351, DOI: 10.1175/2010JCLI3682.1 (2010).

S11. Velicogna, I. and Wahr, J., Measurements of Time-Variable Gravity Show Mass Loss in Antarctica, *Science*, 311:1754–1756, doi:10.1126/science.1123785 (2006).

S12. Peltier, W.R., Closure of the budget of global sea level rise over the GRACE era, *Quat. Sci. Rev.*, do.10.1016j.quascirev.2009.04.004 (2009).

S13. Wu, X., et al., Simultaneous estimation of global present-day water transport and glacial isostatic adjustment, *Nature Geosciences*, 3, 642-646, DOI: 10.1038/NGEO938 (2010).

S14. Rietbroek, R., Brunnabend, S.-E., Kusche, J., Schröter, J., Resolving sea level contributions by identifying fingerprints in time-variable gravity and altimetry, *J. Geodyn*., 59-60, 72-81 (2012).

S15. Vermeersen, L. L. A., and Schotman, H. H. A., Constraints on Glacial Isostatic Adjustment from GOCE and Sea Level Data, *Pure Appl. Geophys*. 166, 1261–1281, DOI 10.1007/s00024-004-0503-3 (2009).

S16. Vinogradova, N. T., Ponte, R. M., Tamisiea, M. E., Quinn, K. J., Hill, E. M., & Davis, J. L., Self-attraction and loading effects on ocean mass redistribution at monthly and longer time scales. *J. Geophys. Res*., 116(C8). doi:10.1029/2011JC007037 (2011).